ORIGINAL RESEARCH

Diacylglycerol Kinase Inhibition Reduces Airway Contraction by Negative Feedback Regulation of Gq-Signaling

Pawan Sharma[1], Santosh K. Yadav[1], Sushrut D. Shah[1], Elham Javed[1], John M. Lim[1], Shi Pan[1], Ajay P. Nayak[1], Reynold A. Panettieri, Jr.[2], Raymond B. Penn[1], Taku Kambayashi[3], and Deepak A. Deshpande[1]

[1]Division of Pulmonary, Allergy, and Critical Care Medicine, Center for Translational Medicine, Jane and Leonard Korman Respiratory Institute, Sidney Kimmel Medical College, Thomas Jefferson University, Philadelphia, Pennsylvania; [2]Rutgers Institute for Translational Medicine and Science, Rutgers, The State University of New Jersey, New Brunswick, New Jersey; and [3]Department of Pathology and Laboratory Medicine, Perelman School of Medicine, University of Pennsylvania, Philadelphia, Pennsylvania

ORCID IDs: 0000-0002-2904-2306 (P.S.); 0000-0001-7375-1698 (S.K.Y.); 0000-0002-6187-5332 (D.A.D.).

Abstract

Exaggerated airway smooth muscle (ASM) contraction regulated by the Gq family of G protein-coupled receptors causes airway hyperresponsiveness in asthma. Activation of Gq-coupled G protein-coupled receptors leads to phospholipase C (PLC)-mediated generation of inositol triphosphate (IP_3) and diacylglycerol (DAG). DAG signaling is terminated by the action of DAG kinase (DGK) that converts DAG into phosphatidic acid (PA). Our previous study demonstrated that DGKζ and α isoform knockout mice are protected from the development of allergen-induced airway hyperresponsiveness. Here we aimed to determine the mechanism by which DGK regulates ASM contraction. Activity of DGK isoforms was inhibited in human ASM cells by siRNA-mediated knockdown of DGKα and ζ, whereas pharmacological inhibition was achieved by pan DGK inhibitor I (R59022). Effects of DGK inhibition on contractile agonist-induced activation of PLC and myosin light chain (MLC) kinase, elevation of IP_3, and calcium levels were assessed. Furthermore, we used precision-cut human lung slices and assessed the role of DGK in agonist-induced bronchoconstriction. DGK inhibitor I attenuated histamine- and methacholine-induced bronchoconstriction. DGKα and ζ knockdown or pretreatment with DGK inhibitor I resulted in attenuated agonist-induced phosphorylation of MLC and MLC phosphatase in ASM cells. Furthermore, DGK inhibition decreased Gq agonist-induced calcium elevation and generation of IP_3 and increased histamine-induced production of PA. Finally, DGK inhibition or treatment with DAG analog resulted in attenuation of activation of PLC in human ASM cells. Our findings suggest that DGK inhibition perturbed the DAG:PA ratio, resulting in inhibition of Gq-PLC activation in a negative feedback manner, resulting in protection against ASM contraction.

Keywords: airway smooth muscle; GPCR; calcium; diacylglycerol kinase; phosphatidic acid

Airway obstruction seen in diseases such as asthma is predominantly driven by an enhanced airway smooth muscle (ASM) response to contractile agonists and is referred to as airway hyperresponsiveness (AHR) (1, 2). Contraction of ASM is promoted primarily by the Gq family of G protein-coupled receptors (GPCRs) (3, 4). Numerous Gq-coupled GPCRs are expressed in ASM, and inflammatory mediators such as histamine, leukotrienes, serotonin, and acetylcholine, whose expression is increased in the asthmatic airways, are agonists of Gq-coupled GPCRs (5). Accordingly, the effectiveness of any one particular Gq-coupled GPCR antagonist as an asthma therapy is likely to be limited (6, 7). Thus, there is a need to focus on a broader downstream target at which Gq-coupled GPCR agonist-mediated contractile signaling in ASM converges.

(Received in original form February 25, 2021; accepted in final form July 22, 2021)

Supported by the National Heart, Lung, and Blood Institute, grants HL146645 (T.K. and D.A.D.), HL137030 (D.A.D.), HL058506 (R.B.P.), PO1HL114471 (R.A.P. and R.B.P.), and ULTR003017 (R.A.P.).

Author Contributions: D.A.D.: conceptualization, project administration, and supervision. P.S., S.K.Y., S.D.S., E.J., J.M.L., S.P., and A.P.N.: data curation, writing, and original draft preparation. R.A.P.: resources. P.S., S.K.Y., S.D.S., J.M.L., S.P., A.P.N., R.A.P., R.B.P., T.K., and D.A.D.: reviewing and editing.

Correspondence and requests for reprints should be addressed to Deepak A. Deshpande, Ph.D., Center for Translational Medicine, Thomas Jefferson University, 1020 Locust Street, JAH 543, Philadelphia, PA 19107-5084. E-mail: Deepak.Deshpande@jefferson.edu.

This article has a related editorial.

Am J Respir Cell Mol Biol Vol 65, Iss 6, pp 658–671, December 2021

Originally Published in Press as DOI: 10.1165/rcmb.2021-0106OC on July 22, 2021
Internet address: www.atsjournals.org

Contractile agonists activate heterotrimeric G proteins in ASM cells followed by the activation of phospholipase C (PLC); PLC converts membrane phospholipid, phosphatidylinositol-4,5-bisphosphate (PIP_2), into inositol trisphosphate (IP_3) and diacylglycerol (DAG) (8–10). IP_3 binds to IP_3 receptors on sarcoplasmic reticulum (SR) and releases calcium (Ca^{2+}) into the cytoplasm (11). Increased Ca^{2+} leads to ASM contraction by promoting phosphorylation of myosin light chain (MLC) mediated by MLC kinase, whereas DAG directly activates protein kinase C (PKC) and downstream signaling cascades, including Ca^{2+} sensitization-mediated regulation of ASM contraction (12). DAG signaling is terminated by the enzyme, DAG kinase (DGK), which converts DAG into phosphatidic acid (PA) (13). Levels of DAG and PA are tightly regulated within the cell, as both of these lipid molecules act as second messengers in numerous cellular processes (14, 15). DGK, therefore, plays a pivotal role in establishing a balance between DAG and PA, and therefore in regulating Gq signaling.

DGKs are ubiquitously expressed and contain at least two cysteine-rich C1 domains (homologous to the DAG binding site of PKC) and a catalytic domain. There are 10 well-characterized mammalian DGK isoforms that can be classified into five different groups: Type I (α, β, γ), II (δ, η, κ), III (ε), IV (ζ, ι), and V (θ) (16). Our recent study has shown that DGKζ (and to a lesser extent DGKα) plays a central role in allergen-induced allergic airway inflammation and development of AHR, and pharmacological targeting of DGK is protective in allergic asthma (17). Interestingly, we found that protection of development of AHR (i.e., exaggerated airway contraction) by DGK isoforms was independent of airway inflammation, but the precise mechanism by which DGK isoforms regulate ASM contraction remains undetermined. Herein, we sought to investigate the mechanism by which DGK inhibition reduces ASM contraction. We tested the effect of inhibition of DGK on the profile of DAG and PA and activation of contractile signaling in human ASM (HASM) cells by Gq-coupled GPCR agonists. Our results indicate that inhibition of DGK perturbs kinetics of DAG and PA (with a decrease in the PA concentration) that in turn inhibits Gq-PLC-IP_3-Ca^{2+}-mediated contractile signaling in ASM in a negative feedback manner. Our study unravels the mechanism through which DGK regulates ASM contraction and, combined with our previous findings from the murine model of asthma, establishes DGK as a potential therapeutic target to provide effective bronchoprotection in asthma.

Methods

Chemicals and Reagents

All standard lab reagents and chemicals were purchased from Sigma unless otherwise mentioned. Anti-pMLC-2 (T18/S19), anti-pMYPT T696 antibody, and RIPA cell lysis buffer were purchased from Cell Signaling Technology. Anti-DGKζ antibody was purchased from Abcam; Anti-DGKα antibody (C-11) was from Santa Cruz. Anti-β-actin antibody was from Sigma. Secondary antibodies, IRDye 680RD or 800CW, were from LI-COR. Diacylglycerol kinase inhibitor I (R59022), acetyl-β-methylcholine chloride, histamine, and other compounds were obtained from Sigma Life Science. 1-Oleoyl-2-acetyl-sn-glycerol (OAG) (catalog number 62600; Cayman Chemical) was purchased from Cayman Chemicals. Protease and phosphatase inhibitors were from Bimake. Insulin-transferrin-selenium (ITS) was from Thermo Fisher Scientific. RhoA Pull-Down Activation Assay Biochem Kit (BK036) was from Cytoskeleton. All polyacrylamide gel casting, running, and transfer reagents and equipment were from Biorad or from previously identified sources (18, 19). SMARTpool: ON-TARGETplus DGKα siRNA and SMARTpool: ON-TARGETplus DGKζ siRNA were obtained from Dharmacon.

Cell Culture

Primary HASM cells were isolated from donor lungs and maintained in culture as described previously (20). HASM cells were used between second to sixth passage and were grown in F-12 media with 10% FBS, penicillin/streptomycin, NaOH, $CaCl_2$, HEPES, and L-Glutamine (Gibco) to confluency and then growth arrested with F-12 supplemented with 1% ITS (growth-arresting media) without serum for 48 hours prior to terminal experiments (21, 22). Cells were pretreated with DGK inhibitor I for 15 minutes, followed by stimulation with an agonist (1 or 10 μM histamine or 10 μM methacholine) for 5, 10, or 15 minutes in general unless otherwise mentioned in the respective experiments. Cell lysates were collected in radioimmunoprecipitation assay (RIPA) buffer. In some experiments, HASM cells immortalized with human telomerase reverse transcriptase (hTERT) were used as described previously (23). In primary HASM cells, expression of m3AChR receptor tends to wane after 2–3 passages, and therefore, hTERT cells that retain expression of m3AChR provide a suitable model to investigate m3AChR signaling.

Transfection of Human ASM Cells

siRNA-mediated knockdown of DGKα or ζ was accomplished as described previously (24). siRNA duplexes for DGK isoforms (ON-TARGET*plus* siRNA SMARTpool) or a scrambled siRNA (ON-TARGET*plus* Non-targeting Control Pool, catalog number D-001810–10–05; Horizon Discovery) were mixed with DharmaFECT 1 Transfection Reagent (catalog number T-2001–01; Horizon Discovery) and subsequently transferred to HASM cells. Twenty-four hours later, cells were passaged for experiments as described below.

HASM cells were cultured in fresh Dulbecco's modified Eagle medium (DMEM) supplemented with 10% FBS and antibiotics and maintained in an incubator at 37°C supplemented with 5% CO_2. cDNA encoding human GFP-C1-PLCδ-PH (Addgene) subcloned into pcDNA3.1 or vector DNA were prepared, and 1 μg plasmid DNA was mixed with 2 μl Lipofectamine 3000 (Invitrogen) in Opti-MEM (Gibco) for 20 minutes. The mixture was then added to the HASM cells as previously described (24, 25). Twelve hours after transfection, cells were serum-starved in growth-arresting media for 24 hours and treated with vehicle or 30 μM DGK inhibitor I for 15 minutes, and then images were obtained by a confocal microscope and analyzed using NIS-Elements AR Version 5.02 software. The transfection efficiency varied between cell cultures from different donors and ranged from 5% to 10%.

Western Blotting

Cells were lysed in RIPA buffer (Cell Signaling Technology) supplemented with protease and phosphatase inhibitor (Bimake) for 20 minutes at 4°C. Lysates were then mixed with Laemmli buffer (Biorad) together with β-mercaptoethanol and boiled at 95°C for 5 minutes. Protein samples were separated on SDS-PAGE and transferred on nitrocellulose membrane. Target proteins

were detected via incubation with respective primary antibodies overnight in 3% BSA containing tris-buffered saline with Tween. Proteins were detected using a secondary antibody conjugated with an infrared dye either at 600 nm or 800 nm wavelength using an Odyssey infrared scanner (LI-COR Biosciences) (26, 27). Protein samples for phospho-myosin light chain (pMLC) and myosin phosphatase target subunit 1 (pMYPT) Western blot analysis were prepared by treating the cells with stop buffer (water:perchloric acid in 1:1 ratio) for 5 minutes on ice after stimulation with respective agonist and then pelleting down the cells by centrifugation. The cell pellet was then washed two times in ice-cold water to remove excess perchloric acid, and then cells were lysed in RIPA buffer followed by denaturation in lithium dodecyl sulfate buffer by boiling at 70°C for 10 minutes. Samples were run on precast gels (Novex) and subsequently transferred onto a nitrocellulose membrane using the mini iBlot system (Invitrogen) (28). Proteins on the membrane were probed using anti-pMLC (catalog number M6068; Sigma), pMYPT (catalog number 4563; Cell Signaling Technology), or anti-β-actin (catalog number A5441; Sigma) antibodies, followed by detection using secondary antibodies conjugated with an infrared dye either at 600 nm or 800 nm wavelength. Intensities of bands were measured using Odyssey infrared imaging software and plotted as a fold change to vehicle-treated samples after normalizing the values with β-actin band intensity. After the second normalization, the statistical analysis was performed by comparing fold change in vehicle- versus DGK inhibitor I-treated cells upon agonist stimulation.

Rho A Activation Assay

Confluent HASM cells on a 10-cm dish were washed with ice-cold PBS and then incubated with 30 μM DGK inhibitor I for 15 minutes, followed by stimulation with 1 μM histamine for 3 minutes in Hanks' balanced salt solution (HBSS). Cells were lysed using a proprietary lysis buffer (catalog number BK036; Cytoskeleton) and subjected to RhoA Pull-Down (Cytoskeleton) for 1 hour at 4°C using beads as per the manufacturer's protocol. Beads were then eluted in Laemmli buffer and subjected to RhoA detection by Western blotting.

Live Cell Imaging

HASM cells were transfected with DNA expressing GFP-C1-PLCδ PH (Addgene) and were then seeded onto 35-mm dishes (MatTek). The cells were then serum-starved in ITS media for 24 hours. Before imaging, cells were washed with HBSS, followed by staining with CellMask Orange actin tracking stain (catalog number A57244; Invitrogen) for 30 minutes at 37°C and 5% CO_2. The CellMask tracker allows the F-actin filaments to be stained without the need for cell permeabilization, as it freely permeates through live cell membranes and can be retained for up to 24 hours in live cells with little to no effect on cell viability. Cells were further washed with HBSS and were then preincubated with either DGK inhibitor I or vehicle for 15 minutes. Baseline images were obtained for 30 seconds using a confocal microscope as previously described (27). GFP fluorescence and actin images were acquired using 40x objective on the Nikon A1R. GFP fluorescence images were obtained for 5 minutes in cells stimulated with vehicle or 1 μM histamine. Actin staining was assessed by taking z-stacks of images before and after histamine stimulation. Change in fluorescence intensity was measured by drawing regions of interest (ROI) on plasma membrane and cytoplasm using NIS-Elements AR Version 5.02 software. All intensity values from confocal microscopy live-cell imaging were plotted against time.

PC-PLC Assay

Immortalized hTERT cells were plated in a 96-well microplate (black clear bottom, density 4–5K cells/well) in cell growth media as described above. Cells were growth arrested in ITS media for 48 hours, pretreated for 15 minutes with 10 μM DGK inhibitor I, and followed by stimulation with 10 μM histamine for 5 minutes. A select set of cells was treated with increasing concentration of OAG (1–500 μM) for 15 minutes, followed by histamine stimulation as described previously (29, 30). The phosphatidylcholine-specific phospholipase C (PC-PLC) activity was determined by using an EnzChek Direct Phospholipase C Assay Kit (Molecular Probes) as per manufacturer's protocol. The assay uses a substrate, glycero-phosphoethanolamine with a dye-labeled sn-2 acyl chain to detect PC-PLC activity. Substrate cleavage by PC-PLC in the cells releases the dye-labeled DAG, producing a positive fluorescence signal measured continuously using a fluorescence microplate reader (Ex:509, Em:516 nm). Absolute PC-PLC activity in HASM cells was calculated by using a standard curve generated using the recombinant PC-PLC enzyme provided in the assay kit.

Inositol Monophosphate Measurement

Primary HASM or hTERT cells were growth arrested in ITS media for 72 hours, pretreated for 15 minutes with DGK inhibitor I, followed by stimulation with 10 μM histamine or 100 μM methacholine (MCh) for 10 minutes. Primary HASM or hTERT cells were transfected with DGKα or ζ siRNA and growth arrested for 72 hours, before stimulation with 10 μM MCh or 10 μM histamine. Cells were lysed, and inositol monophosphate (IP-one or IP) concentrations were measured by using IP-One Gq ELISA (catalog number 72IP1PEA; Cisbio) as described previously (31) and as per the manufacturer's protocol. IP is a metabolite produced following phospholipase C activation and used as a proxy of Gq activation. A standard curve was generated using different concentrations of IP provided by the manufacturer, and the standard curve was used to extrapolate the IP levels in different treatments. IP data are expressed as fold change to IP levels at baseline prior to agonist stimulation.

Calcium Measurement

Growth-arrested primary HASM cells and hTERT cells were incubated with Fluo-4 AM dye (Invitrogen) for 1 hour in a 96-well plate. Cells were treated with vehicle or DGK inhibitor I for 15 minutes while molecular inhibition of DGK was achieved using DGKα or ζ siRNA, and baseline fluorescence was measured for 15 seconds. Subsequently, cells were stimulated with histamine or methacholine and fluorescence was measured in real time for 10 minutes using Flexstation III (Molecular Devices) as described previously (21). The change in the fluorescence values upon agonist stimulation was normalized to maximum change in fluorescence obtained using ionomycin treatment.

Single-cell calcium imaging using confocal microscopy was performed in HASM cells using Fluo-4 calcium indicator dye (Thermo Fischer). Cells were loaded with 5 μM dye for 30 minutes, followed by treatment with DGK inhibitor I for 15 minutes. Confocal dishes were mounted on a Nikon Eclipse Ti2 microscope, and images

were obtained in real time at baseline and following stimulation with histamine, MCh, or KCl until signal stabilized. Fluo-4 intensities were measured using NIS-Elements AR Version 5.02 software by highlighting ROIs and plotted with respect to time.

Phospholipid Quantification

HASM cells were grown to confluency in a 10-cm dish and growth arrested for 24 hours. Cells were washed with PBS, treated with vehicle or DGK inhibitor (30 μM, 15 min) followed by stimulation with 1 μM histamine for 10 minutes. The cell pellet was obtained by scraping the cells from the bottom of the plate in fresh PBS followed by centrifugation. The cell pellet was further processed for lipid extraction and quantification using liquid chromatography–mass spectrometry at the Lipidomics Core Facility, Wayne State University.

Precision-Cut Lung Slices

Human lungs were perfused with 4% low-melting agarose and then sliced using an oscillating tissue slicer (OTS-5000; FHC, Inc.). The lung slices were cultured for 24 hours in Dulbecco's modified Eagle medium supplemented with antimycotic and antibiotic solution at 37°C in a 5% CO_2 incubator. The lung slices were treated with 30 μM DGK inhibitor I for 15 minutes, followed by stimulation with increasing concentration of methacholine (10 nM–10 μM) or histamine (100 nM–100 μM). EVOS FL Auto microscope (Life Technologies) was used to capture images of airways at baseline or at different concentrations of methacholine or histamine, and then area of airway was measured using ImageJ software (National Institutes of Health) for each concentration. Data from lung slice experiments were plotted as percentage of histamine- or methacholine-induced decrease in airway area compared with baseline area.

Statistical Analysis

Data are presented as mean ± SEM from n number of lines derived from different donors. P values were calculated using GraphPad Prism software, with values of $P \leq 0.05$ sufficient to reject the null hypothesis. Unpaired, Student's t test, or one-way ANOVA was applied to determine the effect of DGK inhibition relative to vehicle treatment for various readouts.

Results

DGK Inhibition-reduced Airway Contraction

To assess the potential of DGK inhibition in the regulation of airway contraction, we used human precision-cut lung slices. DGK inhibitor I (R59022) is known to inhibit predominantly DGKα isoform ($IC_{50} = 2.8$ μM) and to a lesser extent DGKζ isoform (32). We used DGK I inhibitor at 10 and 30 μM for 15 minutes (17, 33). Pretreatment of human lung slices with DGK inhibitor I (DGKI, 30 μM, 15 min) reduced contraction to the increasing concentration of contractile agonists, methacholine (1 nM–10 μM; $^*P < 0.05$ at 10 μM) (Figure 1A) and histamine (10 nM–100 μM; $^*P < 0.05$ at 0.5, 1, 10, and 100 μM) (Figure 1B) when compared with vehicle-treated precision-cut lung slices. Interestingly, DGK inhibition had a greater effect on histamine-induced airway contraction compared with methacholine-induced airway contraction.

DGK Inhibition or siRNA-mediated Silencing of DGK Isoforms Reduced Phosphorylation of MLCs

Phosphorylation of MLC facilitates actin–myosin cross-bridge cycling and contraction of ASM. We investigated the effect of DGK inhibition on agonist-induced MLC phosphorylation in HASM cells. Pretreatment of HASM cells with 30 μM DGK inhibitor I significantly reduced phosphorylation of MLC upon stimulation with histamine (1.0 μM, 10 min) compared with vehicle-treated cells (Figures 2A and 2B) ($P < 0.05$).

As mentioned above, there are 10 well-characterized mammalian DGK isoforms, and each isoform of DGK is known to be activated by a unique mechanism providing functional specificity. Calcium binding to EF-hand motifs of DGKα isoform promotes its membrane association and activation, whereas DGKζ isoform possesses a domain homologous to the phosphorylation site domain of the myristoylated alanine-rich C kinase substrate (MARCKS) protein (a substrate for conventional PKCs). Elevation of cytoplasmic calcium concentration activates DGKα and phosphorylation of MARCKS domain of DGKζ by PKC initiates cell signaling mediated through DGKζ pathway (34). Increases in both intracellular calcium levels and PKC activation are involved in Gq-coupled GPCR signaling in ASM. Furthermore, as mentioned above, DGK inhibitor I (R59022) is known to inhibit DGKα predominantly ($IC_{50} = 2.8$ μM) and to a lesser extent DGKζ isoform (32). To further confirm the role of specific isoforms of DGK as mentioned above in the regulation of contractile agonist-induced MLC phosphorylation, we transfected HASM cells with siRNA targeting DGKα or ζ isoform. Transfection of HASM cells with DGKα or ζ siRNA reduced protein expression of each respective isoform when compared with transfection with scrambled siRNA (Figures 2C and 2E). DGKα knockdown significantly reduced phosphorylation of MLC in ASM cells stimulated with 1 μM histamine compared with scrambled siRNA-transfected cells ($P < 0.05$) (Figures 2C and 2D). siRNA knockdown of DGKζ in HASM cells also attenuated 1 μM histamine-induced phosphorylation of MLC compared with scrambled siRNA-transfected cells ($P < 0.05$) (Figure 2E-F). These data suggest that both α and ζ isoforms of DGK regulate contractile signaling in ASM cells. Collectively, pharmacological and genetic studies demonstrate that DGK inhibition diminishes contractile signaling in HASM cells.

Pharmacological and Molecular Inhibition of DGK Reduced Intracellular Calcium Release

ASM contraction and MLC phosphorylation are preceded by increased accumulation of intracellular calcium. Therefore, we investigated the effect of DGK inhibition on agonist-induced calcium elevation in ASM cells. Primary HASM cells maintained in extended culture lose expression of m3AChRs. Therefore, we employed a specific hTERT immortalized HASM cell line previously shown by us to retain robust expression of m3AChR (35). hTERT ASM cells and primary human ASM cells were pretreated with 30 μM DGK inhibitor I, stimulated with either 1 μM histamine or 10 μM MCh or vehicle, and intracellular calcium concentration was measured using the Flexstation III (Molecular Devices) as described in Methods. Treatment with DGK inhibitor I significantly inhibited histamine- and MCh-induced elevation of intracellular calcium concentrations in both hTERT and primary HASM cells (Figures 3A and 3B).

We then validated pharmacological inhibitor results on calcium release with a molecular approach by silencing DGKα or ζ isoform in hTERT and primary HASM cells

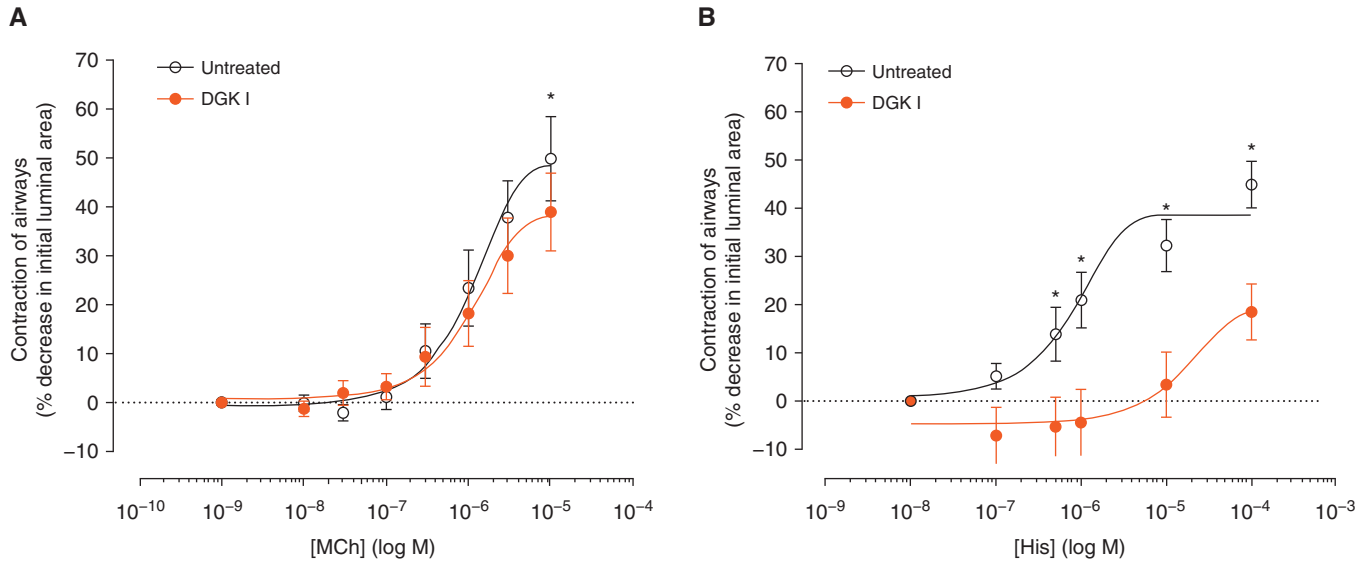

Figure 1. Effect of diacylglycerol kinase (DGK) inhibition on the contraction of human lung slices. Human lung slices were preincubated with 30 μM DGK inhibitor I for 15 minutes, followed by stimulation with an increasing concentration of contractile agonist. (*A* and *B*) Airway area was measured at baseline and after stimulation with methacholine (*A*) and histamine (*B*). Contractile data represent percentage change in luminal area after each agonist stimulation compared with initial luminal area. Red curve represents contraction of airways under DGK inhibition. Data above is mean ± SEM of $n = 6$ independent experiments. *$P < 0.05$ when compared with the vehicle-treated group using ANOVA with Bonferroni *post-hoc* analysis. MCh = methacholine; His = histamine.

(Figures 3C and 3D). Both DGKα and ζ siRNA resulted in significant attenuation of MCh- and histamine-induced calcium release in hTERT ASM cells (Figure 3C). In primary HASM cells, DGKα and ζ siRNA transfection resulted in significant reduction in peak calcium at 10^{-7} and 10^{-6} M histamine (Figure 3D). Furthermore, single-cell intracellular calcium kinetics was studied in primary ASM cells using confocal live-cell microscopy. Again, DGK inhibition significantly ($P < 0.05$) reduced calcium elevation by 10 μM MCh (Figure 3E) and 1 μM histamine (Figure 3F), whereas KCl-induced calcium elevation was not affected by the treatment with DGK inhibitor I (Figure 3G).

DGK Inhibition Reduced Gq-induced Activation of Calcium Sensitization Pathway

Agonist-mediated ASM contraction is sustained (at constant intracellular calcium) by a calcium sensitization pathway mediated by activation of Rho kinase signaling and phosphorylation of MLC phosphatase. Therefore, we measured concentrations of active RhoA (Figure 4A) and phosphorylation of the regulatory subunit of MLC phosphatase (pMYPT1 T696) in HASM cells (Figure 4C). In primary HASM cells, DGK inhibition (30 μM, 15 min) resulted in a significant reduction ($P < 0.05$) of histamine (1 μM)-induced active RhoA compared with vehicle-treated cells (Figures 4A and 4B). Furthermore, both histamine- and methacholine-induced phosphorylation of MYPT (at 10 min) in HASM cells and pretreatment with DGK inhibitor I (30 μM, 15 min) significantly attenuated MYPT phosphorylation (Figures 4C and 4D) ($P < 0.05$).

DGK Inhibition Reduced IP Production and Affected Phospholipid Generation

Elevation of intracellular calcium by contractile agonists in ASM cells is mediated by the PLC-IP_3 cascade. Accumulation of IP, a downstream metabolite of IP_3, following Gq-coupled GPCR activation is used as a readout for Gq activation. Therefore, contractile agonist-induced change in the concentration of IP_3, which is involved in the cellular release of calcium, was indirectly determined using an ELISA for IP. There was a significant reduction of IP concentration following DGK inhibition (30 μM) with both 10 μM histamine and 100 μM methacholine stimulation compared with vehicle-treated cells in both hTERT and primary HASM cells (Figures 5A and 5B). To further confirm the above findings with the pharmacological inhibitor, we used siRNA against DGKα or ζ and measured IP concentrations after stimulation with contractile agonist, MCh (hTERT) (Figure 5C) and histamine (primary ASM) (Figure 5D). Both DGKα and ζ siRNA transfection significantly reduced both MCh- and histamine-induced IP production in HASM cells when compared with cells transfected with scrambled siRNA (Figures 5C and 5D).

After establishing that DGK inhibition prevented agonist-induced IP release, we then investigated its effect on various phospholipid species. It is known that DAG, formed by the hydrolysis of PIP_2 by PLC, is phosphorylated to PA by DAG metabolizing enzyme, DGK (36), and lipid phosphate phosphohydrolases catalyze dephosphorylation of PA to form DAG (37, 38). Also, pharmacological inhibition of DGK modulates stoichiometry of phospholipid molecules, DAG and PA. Therefore, using quantitative liquid chromatography–mass spectrometry, we determined the levels of different species of DAG and PA in HASM cells. A quantitative and unbiased lipidomics analysis captured a wide variety of DAG and PA species in

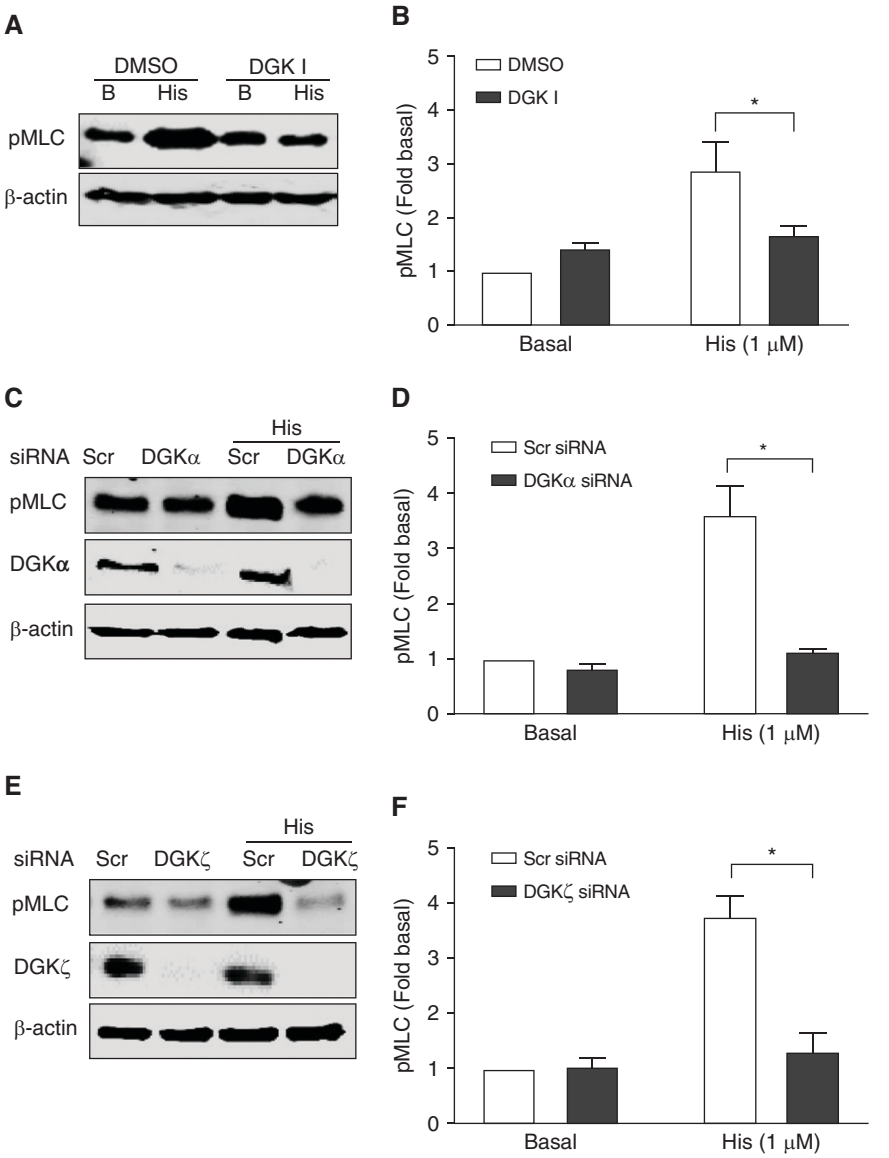

Figure 2. Phosphorylation of myosin light chain (MLC) was reduced by DGK inhibition. Human ASM (HASM) cells were growth arrested with insulin-transferrin-selenium (ITS) media for 72 hours and then treated with 30 μM DGK inhibitor I for 15 minutes, followed by stimulation with 1 μM histamine for 10 minutes. (*A*) Whole cell lysate was obtained as described in METHODS and was subjected to Western blotting using anti-β-actin and pMLC antibody. (*B*) Data from multiple lines of HASM cells is shown in the bar graph. (*C* and *D*) HASM cells were transfected with DGKα siRNA for 72 hours, followed by stimulation with 1 μM histamine for 10 min, and then lysed and probed for pMLC, DGKα and β-actin. (*E* and *F*) DGKζ siRNA-transfected HASM cells were stimulated with 1 μM histamine and then lysed and immunoblotted for pMLC, DGKζ and β-actin. Data above is mean ± SEM of $n = 3$–4 independent experiments. *$P < 0.05$ using one-way ANOVA with Bonferroni *post-hoc* analysis. B = Basal; pMLC = phospho-myosin light chain; Scr = scrambled.

HASM cells (Figures 5E and 5F). Histamine stimulation (1 μM for 15 min) increased total DAG, and DAG concentrations remained unchanged with DGK inhibition I pretreatment while reducing histamine-induced PA accumulation in primary HASM cells. Furthermore, the DAG:PA ratio was calculated using total DAG and PA content in ASM cells under different treatment conditions. Histamine stimulation increased DAG:PA ratio (1.57-fold over basal) in HASM cells, and pretreatment with DGK inhibitor I followed by the stimulation with histamine further significantly increased DAG:PA ratio (2.21-fold over basal). These results suggest the effectiveness of DGK inhibition in modulating phospholipid stoichiometry (decreased PA levels or increased DAG:PA ratio) in HASM cells. Histamine-induced DAG levels did not increase in cells treated with DGK inhibitor, possibly because of inhibition of Gq-PLC signaling.

DGK Inhibition Reduced Agonist-induced PLC Activity

To understand if DGK inhibition has any effect on PLC translocation and activity, we used live cell imaging and PLC assay to answer this puzzling question. Using a PIP_2 selective PH domain as a fluorescent translocation biosensor, we monitored changes in the PLC activation using live-cell confocal microscopy (39). Upon stimulation with a contractile agonist, GFP-PLCδ-PH translocated from the plasma membrane to the cytoplasm. Intensities of GFP in the ROIs were traced on the membrane and in the cytoplasm before and after agonist stimulation in DGK inhibitor- or vehicle- treated cells. Confocal images revealed translocation of GFP-PLCδ-PH in ASM cells upon stimulation with histamine, and GFP translocation was reduced under DGK inhibition compared with vehicle-treated cells, suggesting reduced PLC activation upon DGK inhibition (Figures 6A and 6B). Furthermore, we assessed PLC activity using a fluorescent-based assay. In HASM cells (hTERT), histamine (10 μM) stimulation induced a robust increase in PLC activity, which was attenuated by preincubation with DGK inhibitor I (10 μM) for 15 minutes (Figure 6C). To further test if DGK inhibition-mediated attenuation of PLC activity is due to feedback regulation of PLC activity by DAG, we used a synthetic cell-permeable DAG analog, OAG, to mimic condition of increased DAG. Exogenous addition of OAG dose-dependently inhibited agonist-induced PLC activation with significant effects observed at 300 and 500 μM (Figure 6D).

Collectively, these data suggest that DGK inhibition-induced altered lipid dynamics act in a negative feedback manner to inhibit further activation of PLC-IP_3-calcium signaling in ASM cells (Figure 7).

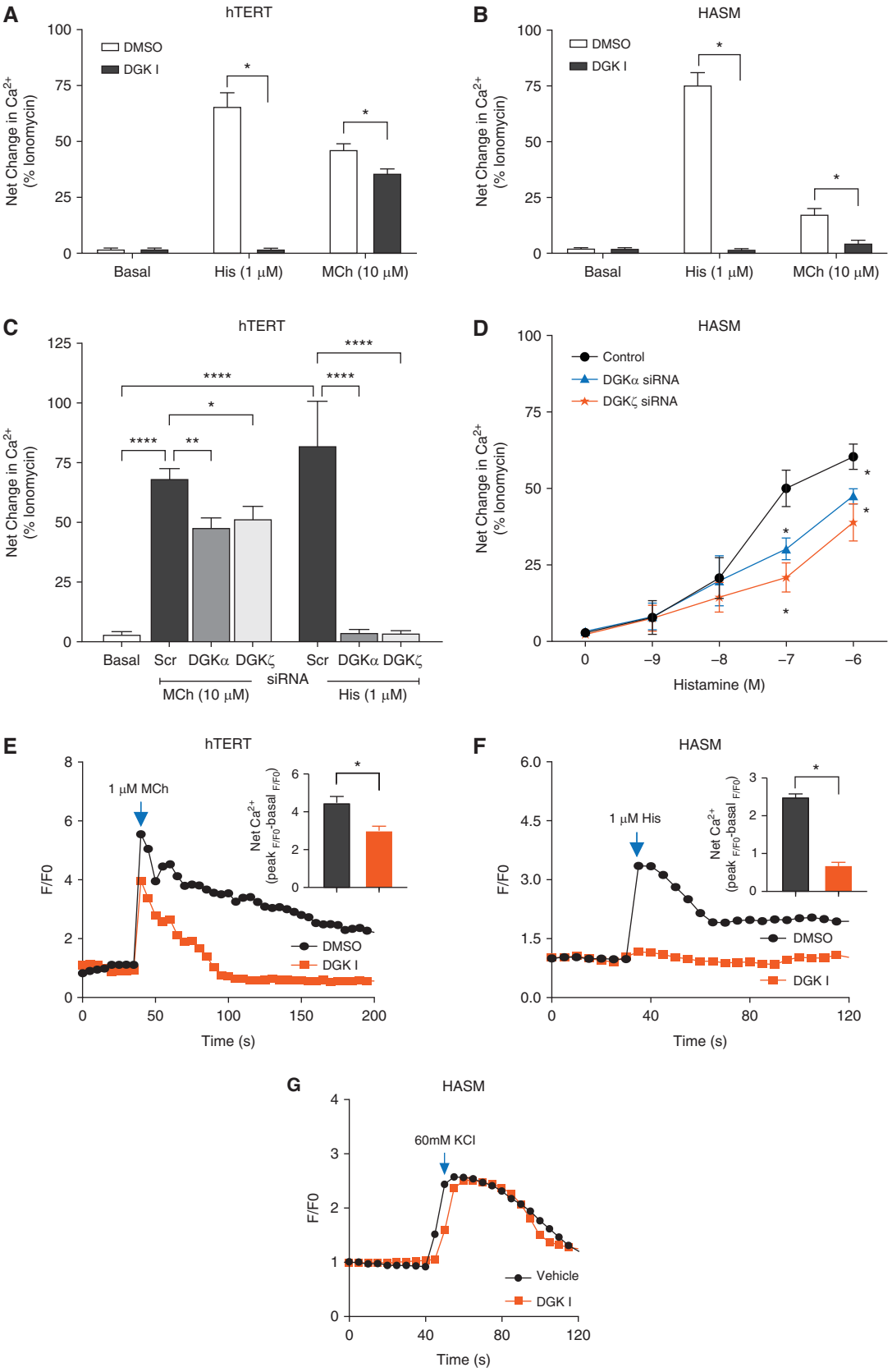

Figure 3. Effect of DGK inhibition on agonist-induced calcium elevation. (*A* and *B*) Immortalized human airway smooth muscle cells (hTERT) (*A*) and primary HASM cells (*B*) were treated with vehicle or DGK inhibitor I (30 μM), and intracellular calcium was measured using Fluo-4 AM dye.

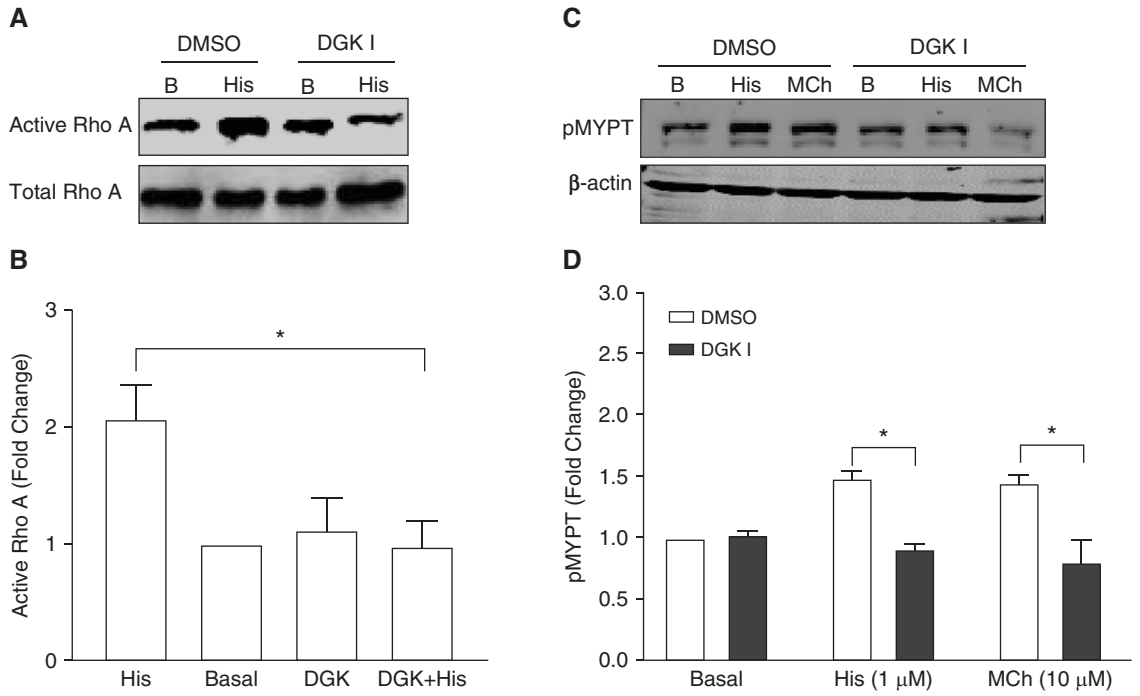

Figure 4. Effect of DGK inhibition on calcium sensitization. (*A* and *B*) Representative Western blot image and graphical representation of densitometric analysis of active RhoA in HASM cells treated with 30 μM DGK inhibitor I for 15 minutes followed by a 10-minute stimulation with 1 μM histamine. (*C* and *D*) HASM cells treated with vehicle or DGK inhibitor I for 15 minutes were stimulated with 1 μM histamine or 10 μM MCh. Cell lysates were subjected to Western blotting for detection of pMYPT. β-Actin was used as a loading control. $*P < 0.05$ using one-way ANOVA with Bonferroni *post-hoc* analysis. ($n = 3$–4). pMYPT = phospho-myosin light chain phosphatase.

Discussion

Asthma pathophysiology is multifactorial, and despite great strides made in the understanding of various phenotypes of asthma, current bronchodilator therapy has limited efficacy in a select cohort of patients with asthma, particularly with chronic use (40, 41). Thus, there is an emerging need for discovering new effective, yet safe, drugs that reduce ASM contraction and promote bronchial relaxation in asthma. We recently identified DGK as a novel target in reducing allergen-induced airway inflammation and AHR in mice (17). Specifically, Singh and colleagues demonstrated diminished allergen-induced airway inflammation (immune cell influx) and reduced Th2 cytokines production together accompanied by abrogation of AHR in DGKζ knockout mice (to a lesser extent in DGKα knockout mice) when compared with wild-type mice. Interestingly, when T cell-specific DGKζ conditional KO mice were challenged with an allergen, only Th2 inflammation but not AHR was reduced, whereas mice with smooth muscle cell-specific deletion of DGKζ exhibited reduced AHR despite having intact airway inflammation upon allergen challenge. These data suggested that inhibition of DGK isoforms in immune cells and ASM cells provides the protection against airway inflammation and AHR respectively.

DGK is expressed in T cells as well as in ASM cells, and DGKζ regulates airway inflammation and ASM contraction in a cell-specific manner (17). However, the mechanism by which DGK inhibition in ASM reduces agonist-induced ASM contraction remains poorly understood. Results from the current study suggest that inhibition of DGK increased DAG:PA ratio and reduced Gq-mediated contractile signaling in human ASM cells by forming a negative feedback loop on PLC activity. We used a cell-permeable DAG analog, OAG, to provide direct evidence that increased DAG is indeed inhibiting PLC activation, resulting in inhibition of ASM contraction. Furthermore, DGK inhibition reduced histamine- or methacholine-induced cytoplasmic IP_3 production with a subsequent reduction in net intracellular calcium ($[Ca^{2+}]_i$) release from SR, preventing phosphorylation of MLC and activation of the calcium-sensitization

Figure 3. (*Continued*). (*C* and *D*) hTERT or HASM cells were transfected with DGKα and ζ siRNA for 72 hours, and agonist-induced intracellular calcium was measured using Fluo-4 AM dye. Cells were stimulated with 10 μM MCh, or 1 μM histamine (*C*) or with increasing concentrations (10^{-9}–10^{-6} M) of histamine (*D*). (*E*–*G*) Single-cell calcium elevation in HASM cells was measured after stimulation of cells with 10 μM MCh (*E*), 1 μM histamine (*F*), or 60 mM KCl (*G*) by confocal live-cell microscopy. Net calcium elevation by histamine or MCh is shown using a bar graph in the insert. Data above is mean ± SEM of $n = 5$–6 independent experiments. $*P < 0.05$, $**P < 0.01$, and $****P < 0.0001$, using one-way ANOVA with Bonferroni *post-hoc* analysis.

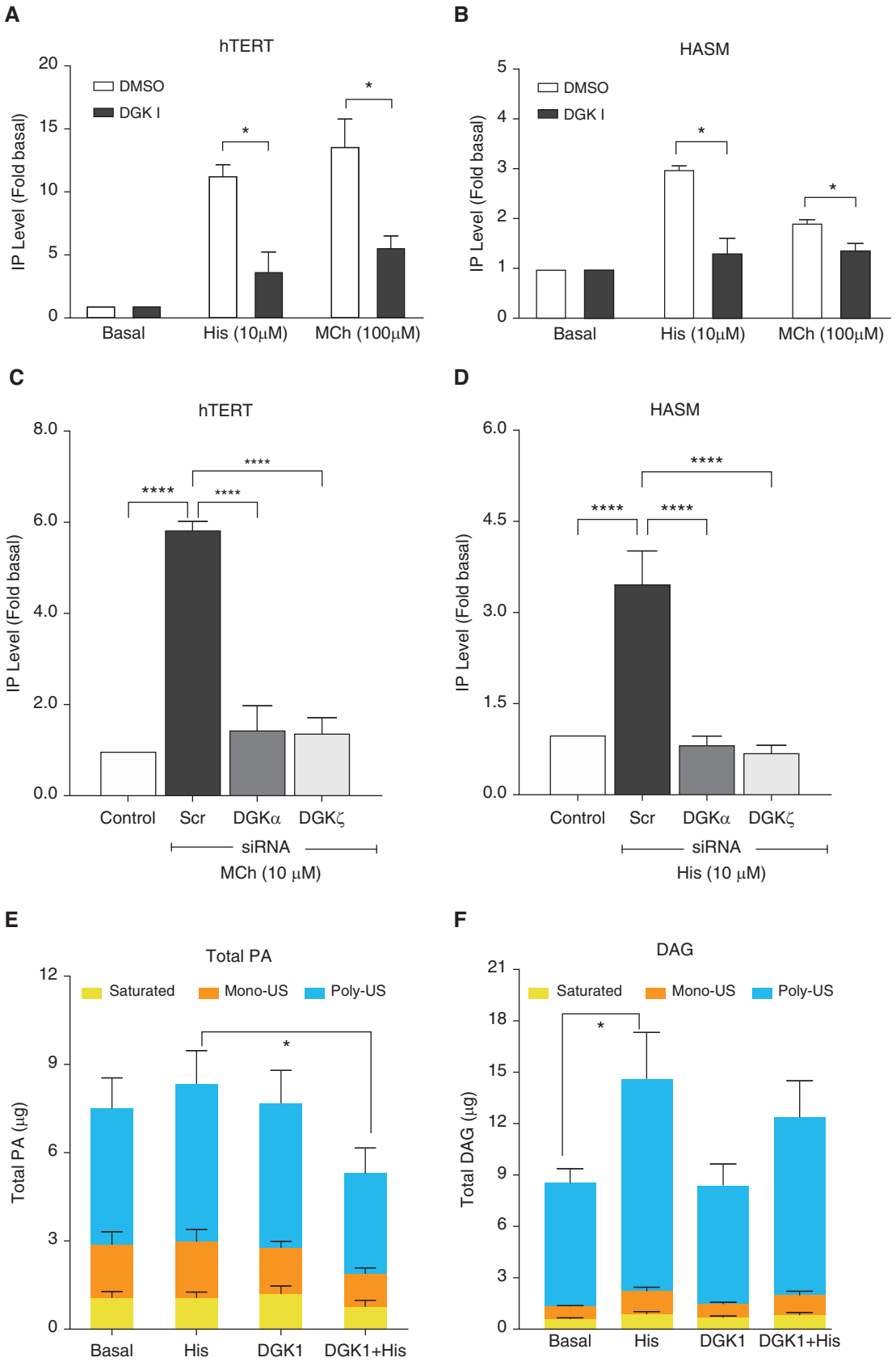

Figure 5. Effect of DGK inhibition on inositol monophosphate (IP) and phospholipid species. hTERT and HASM cells were pretreated with 30 μM DGK inhibitor I for 15 minutes and then stimulated with contractile agonist histamine (10 μM) or MCh (100 μM) for 10 minutes. (*A* and *B*)

mechanism, resulting in reduced ASM contraction (Figure 7).

Increased intrinsic mechanical properties and greater responsiveness to contractile agonists are important determinants of bronchoconstriction in asthma (42, 43). Discovering novel regulatory mechanisms of Gq signaling that impact ASM function is an attractive avenue for antiasthma drugs. Current strategies include the use of muscarinic and leukotriene receptor antagonists; however, these drugs demonstrate a limited clinical efficacy as multiple Gq-coupled receptor subtypes contribute to various airway-related pathologies. Hence a broader approach by inhibiting Gq activation may be advantageous. This notion is supported by recent studies demonstrating the prorelaxant capacity of the pharmacological Gq inhibitor, YM-254890 (7, 44). Additionally, inhibition of PLC-β is another potential approach as this enzyme is activated by Gq-coupled GPCRs (45). Gαq regulation of PLC-β–mediated activation of downstream effectors has been successfully demonstrated using a fusion peptide derived from a helix–turn–helix region of PLC-β3 (the critical region for interaction with Gαq), leading to inhibition of PLC activation (46). This peptide inhibited PLC activation by Gαq in reconstituted lipid vesicles and inhibited Gαq signaling in cells (47). Our previous study demonstrated that both pharmacological inhibition and genetic ablation of DGK isoform protected against development of AHR (17). Our results in the current study consolidate the previous findings by Singh and colleagues and establish DGK as a therapeutic target to reduce ASM contraction.

The current study investigated the potential of DGK inhibition in mitigating airway contraction, representing the first study to comprehensively investigate the role of DGK in the regulation of contractile signaling in ASM cells. Expression and function of various DGK enzymes have been investigated in vascular smooth muscle (48), where pharmacological inhibition of DGK has been shown to attenuate Gq-coupled GPCR agonist-induced vascular smooth muscle (aorta and coronary artery) contraction (48, 49). In this study, we have comprehensively investigated the effect of DGK inhibition on ASM contractile signaling and have elucidated the mechanism by which DGK inhibition affects agonist-mediated ASM contraction. These differences could result from different subcellular localization of signaling molecules that are important for regulating contractile signaling in ASM, such as lipid rafts and the receptor reserve associated with contractile agonist-mediated signaling (50–53). Studies have shown that lipid rafts are key sites for signal transduction owing to their high content of signaling proteins such as GPCRs, heterotrimeric and small G proteins, and PKC (45, 54). Therefore, differences in the morphology and associated proteins in the lipid rafts suggest that these domains do serve as distinct or complementary functions in ASM cells, which warrants further investigation in the context of DGK inhibition (45).

One of the novel findings of our study that may eventually dictate bronchoprotection in asthma is that DGK inhibition reduced the phosphorylation of MLC in HASM cells. Furthermore, this reduction of MLC phosphorylation under contractile agonist stimulation was sustained under DGKα and DGKζ knockdown condition, which implies that both α and ζ isoforms of DGK are essential in promoting receptor mediated ASM contraction. It is also known that the DGKα isoform is activated directly by an increase in the $[Ca^{2+}]_i$ concentrations, whereas DGKζ is activated by PKC-mediated phosphorylation of the MARCKS domain (34). Notably, increases in both $[Ca^{2+}]_i$ concentrations and PKC activation are involved in Gq-coupled GPCR signaling in ASM (5). MLC phosphorylation is regulated by calcium-calmodulin-activated MLC kinase and Rho-Rac–activated MLC phosphatase (55), both of which are attenuated by DGK inhibition in this study.

DGK is involved in conversion of DAG to PA, and inhibition of DGK leads to accumulation of DAG, which acts as a negative feedback signal to reduce PLC activity (Figure 7). Inhibition of DGKζ was associated with a decreased antigen (FcεRI)-induced calcium response in the RBL-2H3 mast cell line, although the studies revealed no effect on PLC activity (56). A role of DGK in establishing a negative feedback loop has been shown in other conditions such as long-term potentiation and mast cell degranulation, where DGKζ interaction with PKCα reduced PKCα activity and promoted DAG metabolism (57). On the other hand, regulation of PKCα by DGKζ is attenuated by PKCα-dependent phosphorylation of DGKζ and by subsequent dissociation of PKCα from DGKζ, thereby fine-tuning PKCα for diverse cellular functions (57, 58). Interaction between DGK isoforms and PKC appears to be spatiotemporally restricted, thereby forming signaling nodes. Future studies are needed to explore additional mechanisms that regulate PKC-mediated activation of downstream targets relevant to ASM contraction.

In summary, our findings support the novel idea that DGK inhibition provides protection against ASM contraction as seen with exaggerated ASM narrowing in asthma. This study also elucidated the mechanism(s) by which DGK inhibition may actually work in reducing receptor-mediated contraction of

Figure 5. (*Continued*). IP concentrations were measured by ELISA as described in METHODS. DGK inhibition attenuated histamine and MCh-induced IP concentrations in hTERT (*A*) and HASM (*B*) cells. (*C* and *D*) Similarly, IP concentrations were measured in hTERT or HASM cells transfected with DGKα and ζ siRNA for 72 hours, followed by stimulation with 10 μM MCh (*C*) or 10 μM histamine (His) for 10 min (*D*). Data above is mean ± SEM of $n = 5$ independent experiments. $^*P < 0.05$ and $^{****}P < 0.0001$, using one-way ANOVA with Bonferroni *post-hoc* analysis. (*E* and *F*) Lipidomics analysis revealed presence of multiple species of phospholipids. HASM cells treated with vehicle or DGK inhibitor I were stimulated with histamine, and phospholipids were quantified using a liquid chromatography–mass spectrometry method. Quantitative liquid chromatography–mass spectrometry analysis revealed multiple species of PA (*E*) and DAG (*F*) at baseline and upon agonist stimulation (1 μM histamine, 10 min). DGK inhibition (30 μM DGKI, 15 min) reduced agonist-induced PA levels (*D*). $^*P < 0.05$, using one-way ANOVA with Bonferroni *post-hoc* analysis. $n = 4$. US = unsaturated.

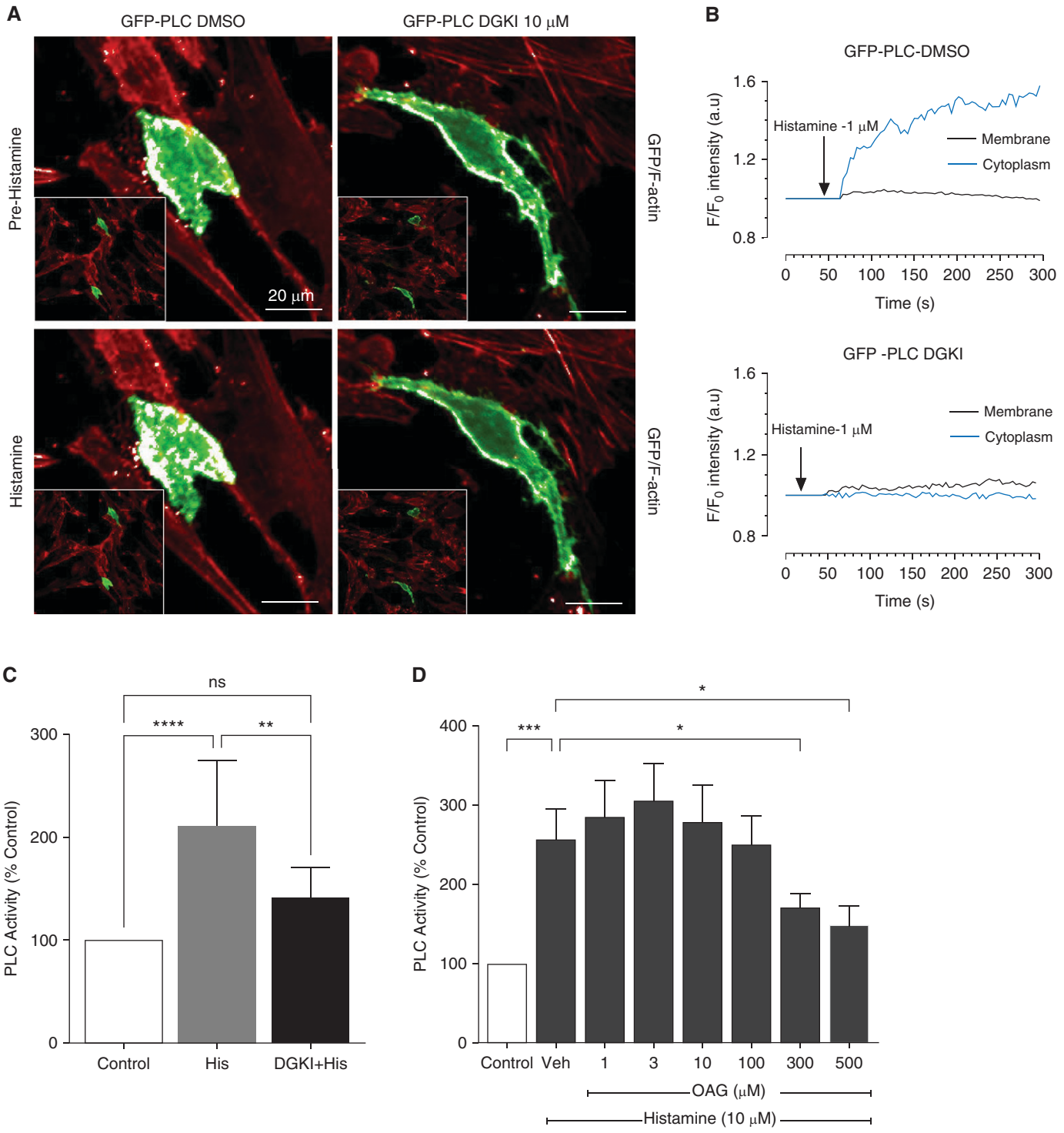

Figure 6. Effect of DGK inhibition on phospholipase C (PLC) activation. HASM cells were transfected with GFP-PLCδ-PH domain and then growth arrested for 24 hours in ITS medium. Cells were treated with histamine, and localization of GFP was measured using a Nikon confocal microscope. (*A*) GFP intensity was measured by drawing a region of interest on the membrane and in the cytoplasm. Scale bars, 20 μm. (*B*) Intensity tracing was done by plotting values using GraphPad. (*C*) hTERT were used to measure PLC activity at baseline and after treatment with histamine for 5 minutes (±10 μM DGK inhibitor I, 15 min). Cells were treated with a cell-permeable DAG analog, 1-oleoyl-2-acetyl-sn-glycerol (1–500 μM), followed by stimulation with histamine, and PLC activity in whole-cell lysate was determined as described in Methods (*D*). *$P<0.05$, **$P<0.01$, ***$P<0.001$, and ****$P<0.0001$, using one-way ANOVA with Bonferroni *post-hoc* analysis. (C) $n=4$; (D) $n=5$.

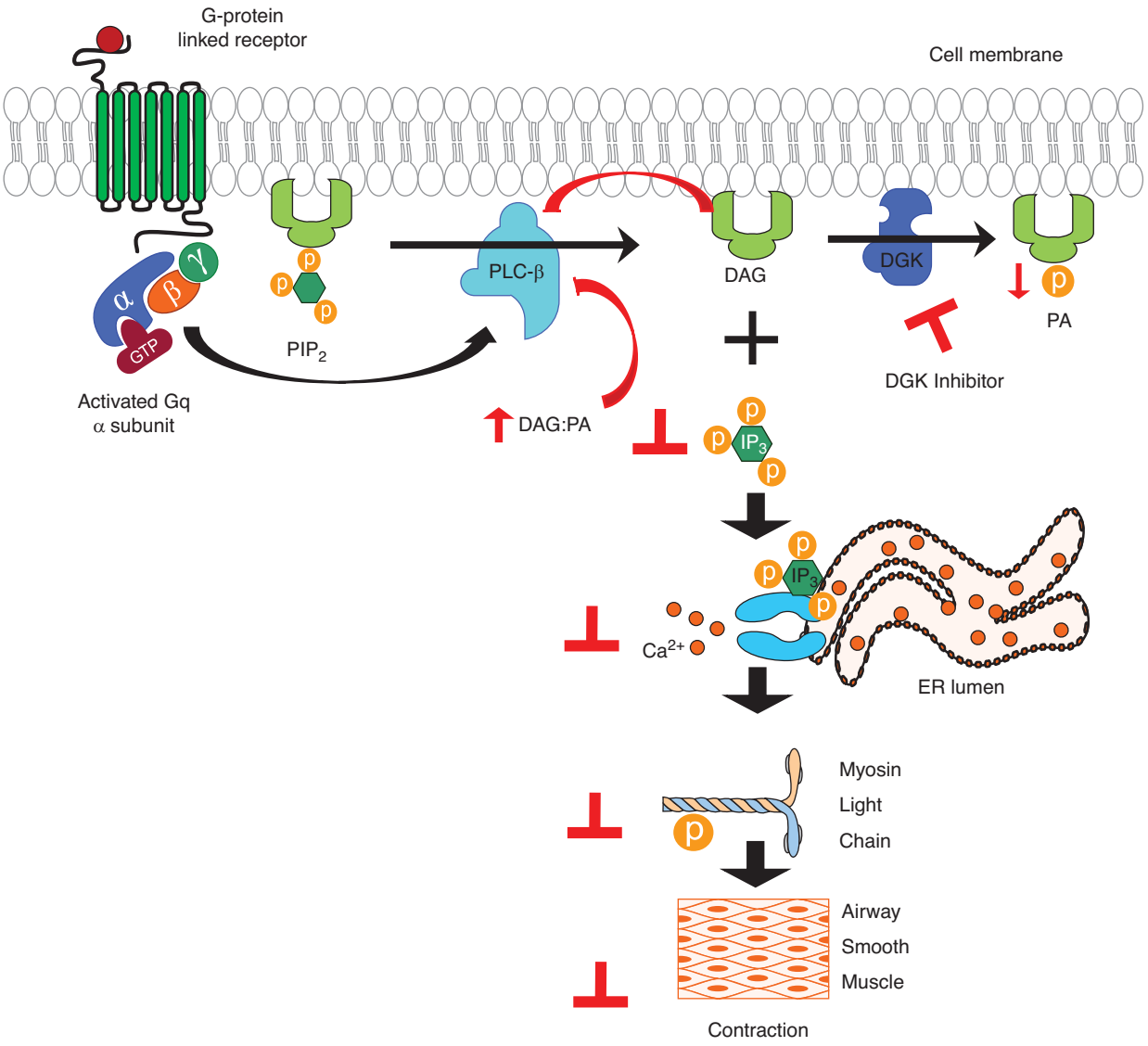

Figure 7. Model depicting the mechanism by which DGK inhibition regulates ASM contraction. DGK inhibition (shown in red) leads to decreased conversion of DAG to PA and forms a negative feedback loop on PLC activity, which reduces IP_3 production and calcium release into the cytosol and ultimately leads to reduced phosphorylation of MLC required for cross-bridging with actin and thus reducing contraction.

ASM with a pathophysiological significance in asthma. Thus, our study further provides key mechanistic insight into previous findings that DGK inhibition mitigates the asthma phenotype *in vivo*. We submit that pharmacological targeting of DGK may be a viable option in relieving broncho- constriction in asthma, and our study lays the foundation for discovering highly effective and safe DGK inhibitors for other obstructive lung diseases. ■

Author disclosures are available with the text of this article at www.atsjournals.org.

Acknowledgment: The authors thank the Lipidomics Core Facility at Wayne State University, Detroit, for assistance with the lipidomics analysis.

References

1. Woolcock AJ, Salome CM, Yan K. The shape of the dose-response curve to histamine in asthmatic and normal subjects. *Am Rev Respir Dis* 1984; 130:71–75.
2. Palmqvist M, Pettersson K, Sjöstrand M, Andersson B, Löwhagen O, Lötvall J. Mild experimental exacerbation of asthma induced by individualised low-dose repeated allergen exposure. A double-blind evaluation. *Respir Med* 1998;92:1223–1230.
3. Penn RB, Bond RA, Walker JK. GPCRs and arrestins in airways: implications for asthma. *Handb Exp Pharmacol* 2014;219: 387–403.
4. Deshpande DA, Penn RB. Targeting G protein-coupled receptor signaling in asthma. *Cell Signal* 2006;18:2105–2120.

5. Billington CK, Penn RB. Signaling and regulation of G protein-coupled receptors in airway smooth muscle. *Respir Res* 2003;4:2.
6. Bradley SJ, Wiegman CH, Iglesias MM, Kong KC, Butcher AJ, Plouffe B, *et al.* Mapping physiological G protein-coupled receptor signaling pathways reveals a role for receptor phosphorylation in airway contraction. *Proc Natl Acad Sci USA* 2016;113:4524–4529.
7. Matthey M, Roberts R, Seidinger A, Simon A, Schröder R, Kuschak M, *et al.* Targeted inhibition of G_q signaling induces airway relaxation in mouse models of asthma. *Sci Transl Med* 2017;9:eaag2288.
8. Essen LO, Perisic O, Katan M, Wu Y, Roberts MF, Williams RL. Structural mapping of the catalytic mechanism for a mammalian phosphoinositide-specific phospholipase C. *Biochemistry* 1997;36:1704–1718.
9. Penn RB, Benovic JL. Regulation of heterotrimeric G protein signaling in airway smooth muscle. *Proc Am Thorac Soc* 2008;5:47–57.
10. Sternweis PC, Smrcka AV. Regulation of phospholipase C by G proteins. *Trends Biochem Sci* 1992;17:502–506.
11. Hall IP. Second messengers, ion channels and pharmacology of airway smooth muscle. *Eur Respir J* 2000;15:1120–1127.
12. Carrasco S, Merida I. Diacylglycerol-dependent binding recruits PKCtheta and RasGRP1 C1 domains to specific subcellular localizations in living T lymphocytes. *Mol Biol Cell* 2004;15:2932–2942.
13. Cai J, Abramovici H, Gee SH, Topham MK. Diacylglycerol kinases as sources of phosphatidic acid. *Biochim Biophys Acta* 2009;1791:942–948.
14. Mérida I, Avila-Flores A, Merino E. Diacylglycerol kinases: at the hub of cell signalling. *Biochem J* 2008;409:1–18.
15. Takai Y, Kishimoto A, Kikkawa U, Mori T, Nishizuka Y. Unsaturated diacylglycerol as a possible messenger for the activation of calcium-activated, phospholipid-dependent protein kinase system. 1979. *Biochem Biophys Res Commun* 2012;425:571–577.
16. van Blitterswijk WJ, Houssa B. Properties and functions of diacylglycerol kinases. *Cell Signal* 2000;12:595–605.
17. Singh BK, Lu W, Schmidt Paustian AM, Ge MQ, Koziol-White CJ, Flayer CH, *et al.* Diacylglycerol kinase ζ promotes allergic airway inflammation and airway hyperresponsiveness through distinct mechanisms. *Sci Signal* 2019;12:eaax3332.
18. Sharma P, Panebra A, Pera T, Tiegs BC, Hershfeld A, Kenyon LC, *et al.* Antimitogenic effect of bitter taste receptor agonists on airway smooth muscle cells. *Am J Physiol Lung Cell Mol Physiol* 2016;310:L365–L376.
19. Michael JV, Gavrila A, Nayak AP, Pera T, Liberato JR, Polischak SR, *et al.* Cooperativity of E-prostanoid receptor subtypes in regulating signaling and growth inhibition in human airway smooth muscle. *FASEB J* 2019;33:4780–4789.
20. Panettieri RA, Murray RK, DePalo LR, Yadvish PA, Kotlikoff MI. A human airway smooth muscle cell line that retains physiological responsiveness. *Am J Physiol* 1989;256:C329–C335.
21. Deshpande DA, Wang WC, McIlmoyle EL, Robinett KS, Schillinger RM, An SS, *et al.* Bitter taste receptors on airway smooth muscle bronchodilate by localized calcium signaling and reverse obstruction. *Nat Med* 2010;16:1299–1304.
22. Pulkkinen V, Manson ML, Säfholm J, Adner M, Dahlén SE. The bitter taste receptor (TAS2R) agonists denatonium and chloroquine display distinct patterns of relaxation of the guinea pig trachea. *Am J Physiol Lung Cell Mol Physiol* 2012;303:L956–L966.
23. Sharma P, Tran T, Stelmack GL, McNeill K, Gosens R, Mutawe MM, *et al.* Expression of the dystrophin-glycoprotein complex is a marker for human airway smooth muscle phenotype maturation. *Am J Physiol Lung Cell Mol Physiol* 2008;294:L57–L68.
24. Saxena H, Deshpande DA, Tiegs BC, Yan H, Battafarano RJ, Burrows WM, *et al.* The GPCR OGR1 (GPR68) mediates diverse signalling and contraction of airway smooth muscle in response to small reductions in extracellular pH. *Br J Pharmacol* 2012;166:981–990.
25. Stauffer TP, Ahn S, Meyer T. Receptor-induced transient reduction in plasma membrane PtdIns(4,5)P2 concentration monitored in living cells. *Curr Biol* 1998;8:343–346.
26. Deshpande DA, Yan H, Kong KC, Tiegs BC, Morgan SJ, Pera T, *et al.* Exploiting functional domains of GRK2/3 to alter the competitive balance of pro- and anticontractile signaling in airway smooth muscle. *FASEB J* 2014;28:956–965.
27. Pan S, Sharma P, Shah SD, Deshpande DA. Bitter taste receptor agonists alter mitochondrial function and induce autophagy in airway smooth muscle cells. *Am J Physiol Lung Cell Mol Physiol* 2017;313:L154–L165.
28. Yoo EJ, Cao G, Koziol-White CJ, Ojiaku CA, Sunder K, Jude JA, *et al.* $G\alpha_{12}$ facilitates shortening in human airway smooth muscle by modulating phosphoinositide 3-kinase-mediated activation in a RhoA-dependent manner. *Br J Pharmacol* 2017;174:4383–4395.
29. Tu P, Kunert-Keil C, Lucke S, Brinkmeier H, Bouron A. Diacylglycerol analogues activate second messenger-operated calcium channels exhibiting TRPC-like properties in cortical neurons. *J Neurochem* 2009;108:126–138.
30. Andoh T, Itoh H, Watanabe I, Sasaki T, Higashi T. Mechanisms of modulation of neuronal nicotinic receptors by substance P and OAG. *Am J Physiol Cell Physiol* 2001;281:C1871–C1880.
31. Trinquet E, Bouhelal R, Dietz M. Monitoring Gq-coupled receptor response through inositol phosphate quantification with the IP-One assay. *Expert Opin Drug Discov* 2011;6:981–994.
32. de Chaffoy de Courcelles DC, Roevens P, van Belle H. R 59 022, a diacylglycerol kinase inhibitor. Its effect on diacylglycerol and thrombin-induced C kinase activation in the intact platelet. *J Biol Chem* 1985;260:15762–15770.
33. Martinez K, Shyamasundar S, Kennedy A, Chuang CC, Marsh A, Kincaid J, *et al.* Diacylglycerol kinase inhibitor R59022 attenuates conjugated linoleic acid-mediated inflammation in human adipocytes. *J Lipid Res* 2013;54:662–670.
34. Shulga YV, Topham MK, Epand RM. Regulation and functions of diacylglycerol kinases. *Chem Rev* 2011;111:6186–6208.
35. Pera T, Deshpande DA, Ippolito M, Wang B, Gavrila A, Michael JV, *et al.* Biased signaling of the proton-sensing receptor OGR1 by benzodiazepines. *FASEB J* 2018;32:862–874.
36. Welti R, Li W, Li M, Sang Y, Biesiada H, Zhou HE, *et al.* Profiling membrane lipids in plant stress responses. Role of phospholipase D alpha in freezing-induced lipid changes in Arabidopsis. *J Biol Chem* 2002;277:31994–32002.
37. Brindley DN, Waggoner DW. Mammalian lipid phosphate phosphohydrolases. *J Biol Chem* 1998;273:24281–24284.
38. Delon C, Manifava M, Wood E, Thompson D, Krugmann S, Pyne S, *et al.* Sphingosine kinase 1 is an intracellular effector of phosphatidic acid. *J Biol Chem* 2004;279:44763–44774.
39. Szentpetery Z, Balla A, Kim YJ, Lemmon MA, Balla T. Live cell imaging with protein domains capable of recognizing phosphatidylinositol 4,5-bisphosphate; a comparative study. *BMC Cell Biol* 2009;10:67.
40. Bond RA. Is paradoxical pharmacology a strategy worth pursuing? *Trends Pharmacol Sci* 2001;22:273–276.
41. Rabe KF, Adachi M, Lai CK, Soriano JB, Vermeire PA, Weiss KB, *et al.* Worldwide severity and control of asthma in children and adults: the global asthma insights and reality surveys. *J Allergy Clin Immunol* 2004;114:40–47.
42. Prakash YS. Emerging concepts in smooth muscle contributions to airway structure and function: implications for health and disease. *Am J Physiol Lung Cell Mol Physiol* 2016;311:L1113–L1140.
43. An SS, Bai TR, Bates JH, Black JL, Brown RH, Brusasco V, *et al.* Airway smooth muscle dynamics: a common pathway of airway obstruction in asthma. *Eur Respir J* 2007;29:834–860.
44. Carr R III, Koziol-White C, Zhang J, Lam H, An SS, Tall GG, *et al.* Interdicting Gq activation in airway disease by receptor-dependent and receptor-independent mechanisms. *Mol Pharmacol* 2016;89:94–104.
45. Sharma P, Ghavami S, Stelmack GL, McNeill KD, Mutawe MM, Klonisch T, *et al.* beta-Dystroglycan binds caveolin-1 in smooth muscle: a functional role in caveolae distribution and Ca2+ release. *J Cell Sci* 2010;123:3061–3070.
46. Campbell AP, Smrcka AV. Targeting G protein-coupled receptor signalling by blocking G proteins. *Nat Rev Drug Discov* 2018;17:789–803.
47. Lyon AM, Tesmer JJ. Structural insights into phospholipase C-β function. *Mol Pharmacol* 2013;84:488–500.
48. Choi H, Allahdadi KJ, Tostes RC, Webb RC. Diacylglycerol kinase inhibition and vascular function. *Curr Enzym Inhib* 2009;5:148–152.
49. Ohanian J, Heagerty AM. Membrane-associated diacylglycerol kinase activity is increased by noradrenaline, but not by angiotensin II, in arterial smooth muscle. *Biochem J* 1994;300:51–56.
50. Sprong H, van der Sluijs P, van Meer G. How proteins move lipids and lipids move proteins. *Nat Rev Mol Cell Biol* 2001;2:504–513.

51. Wood MD, Murkitt KL, Ho M, Watson JM, Brown F, Hunter AJ, *et al.* Functional comparison of muscarinic partial agonists at muscarinic receptor subtypes hM1, hM2, hM3, hM4 and hM5 using microphysiometry. *Br J Pharmacol* 1999;126:1620–1624.
52. Gunst SJ, Stropp JQ, Flavahan NA. Muscarinic receptor reserve and beta-adrenergic sensitivity in tracheal smooth muscle. *J Appl Physiol (1985)* 1989;67:1294–1298.
53. Sharma P, Ryu MH, Basu S, Maltby SA, Yeganeh B, Mutawe MM, *et al.* Epithelium-dependent modulation of responsiveness of airways from caveolin-1 knockout mice is mediated through cyclooxygenase-2 and 5-lipoxygenase. *Br J Pharmacol* 2012;167: 548–560.
54. Razani B, Woodman SE, Lisanti MP. Caveolae: from cell biology to animal physiology. *Pharmacol Rev* 2002;54:431–467.
55. Kaneko-Kawano T, Takasu F, Naoki H, Sakumura Y, Ishii S, Ueba T, *et al.* Dynamic regulation of myosin light chain phosphorylation by Rho-kinase. *PLoS One* 2012;7:e39269.
56. Sakuma M, Shirai Y, Ueyama T, Saito N. Diacylglycerol kinase γ regulates antigen-induced mast cell degranulation by mediating Ca(2+) influxes. *Biochem Biophys Res Commun* 2014;445: 340–345.
57. Luo B, Prescott SM, Topham MK. Protein kinase C alpha phosphorylates and negatively regulates diacylglycerol kinase zeta. *J Biol Chem* 2003; 278:39542–39547.
58. Lee D, Yamamoto Y, Kim E, Tanaka-Yamamoto K. Functional and physical interaction of diacylglycerol kinase ζ with protein kinase Cα is required for cerebellar long-term depression. *J Neurosci* 2015;35: 15453–15465.